

# Direct Observation of Methyl Radicals Islanding on Copper Surface and Its Effects on the Kinetics of Catalytic Reactions

Yuet Loy Chan, Woei Wu Pai, and Tung J. Chuang\*

Center for Condensed Matter Sciences, National Taiwan University, Taipei 106, Taiwan

Received: September 30, 2003

The formation of methyl radicals into densely packed two-dimensional islands on the Cu(111) surface is directly observed for the first time by scanning tunneling microscopy (STM). It is shown that chemisorbed  $\text{CH}_3(\text{ads})$  molecules tend to aggregate into  $(\sqrt{3} \times \sqrt{3}) \text{R}30^\circ$  structure in 2D islands at any coverage up to one saturation monolayer. The island sizes depend on the amount of gaseous exposure, and at a given exposure, the sizes are found to decrease when the surface temperature is raised to near the reaction temperature of  $\text{CH}_3(\text{ads})$ . The adsorbate islanding behavior can be correlated with the first-order reaction kinetics in the generation of long-chain alkene products detected in the thermal desorption. From this and other related studies on methyl–solid interactions, we infer that the islanding phenomenon may be quite general in catalytic systems.

## Introduction

There are increasing reports in surface chemistry concerning the islanding behavior of adsorbates and its effect on the reaction processes.<sup>1–5</sup> It appears, however, that in hydrocarbon surface catalysis, the islanding phenomenon of  $\text{CH}_x$  radicals and its correlation with the chain propagation reactions have rarely been investigated. Recently, there are many experimental and theoretical studies devoted to uncovering the basic reaction steps and mechanisms involving heterogeneous catalysis of hydrocarbons.<sup>6–8</sup> A number of recent investigations<sup>8–17</sup> have shown remarkably that long chain hydrocarbons can be produced from  $\text{CH}_3$  groups adsorbed on single-crystal surfaces by thermal activation under ultrahigh vacuum (UHV) conditions, resembling important aspects of the well-known Fischer–Tropsch synthesis in atmospheric environments. It has been suggested from the studies<sup>8–14</sup> that the chain reactions are initiated by the dehydrogenation of chemisorbed  $\text{CH}_3(\text{ads})$  to generate  $\text{CH}_2(\text{ads})$ , which subsequently interacts with  $\text{CH}_3(\text{ads})$  by  $\alpha$ -insertion to yield  $\text{C}_{2+}$  alkanes. Namely, the reaction scheme can be represented by  $\text{CH}_3(\text{ads}) \rightarrow \text{CH}_2(\text{ads}) + \text{H}(\text{ads})$ , followed by  $\text{CH}_3(\text{ads}) + \text{CH}_2(\text{ads}) \rightarrow \text{C}_2\text{H}_5(\text{ads}) \rightarrow \text{C}_2\text{H}_4(\text{g})\uparrow + \text{H}(\text{ads})$  and  $\text{C}_2\text{H}_5(\text{ads}) + \text{CH}_2(\text{ads}) \rightarrow \text{C}_3\text{H}_7(\text{ads}) \rightarrow \text{C}_3\text{H}_6(\text{g})\uparrow + \text{H}(\text{ads})$ , etc., chain reactions. This reaction mechanism is supported by the product distributions detected in temperature-programmed desorption (TPD) for  $\text{CH}_3(\text{ads})$  not only on various faces of Cu crystals<sup>8–12</sup> but also on oxygen-modified Mo surface<sup>13,14</sup> and NiO.<sup>15</sup> It is very surprising to observe, however, that the series of high-mass alkene products (from  $\text{C}_2\text{H}_4$  to as high as  $\text{C}_5\text{H}_{10}$  in some instances) are generated and desorbed from the catalytic surfaces all at the same temperature and independent of surface coverages.<sup>9–17</sup> Apparently, the chain reactions involve many sequential C–C group couplings, but they all exhibit first-order reaction kinetics with the  $\text{C}_{2+}$  product yields dependent linearly only on the initial surface concentration of methyl radicals,  $[\text{CH}_3(\text{ads})]$ . Yet according to the chemical equations outlined above, the reaction rate to generate  $\text{C}_2\text{H}_4(\text{g})$  should be proportional to both  $[\text{CH}_3(\text{ads})]$  and  $[\text{CH}_2(\text{ads})]$  and that for  $\text{C}_3\text{H}_6(\text{g})$  should

depend on  $[\text{CH}_3(\text{ads})]$  and  $[\text{CH}_2(\text{ads})]^2$ . In other words, the yields for  $\text{C}_2\text{H}_4$ ,  $\text{C}_3\text{H}_6$ , and higher-mass alkene products should be proportional to  $[\text{CH}_3(\text{ads})]^n$  with  $n > 1$ . Furthermore, the TPD peak shapes and temperatures should vary with  $\text{CH}_3(\text{ads})$  surface concentration. These expected TPD characteristics based on the chemical equations are in drastic contradiction to the experimental observation. It is known that for first-order kinetics to be operative in a coupling chain reaction, the reactants cannot afford to take time-consuming diffusion steps if they are adsorbed far apart on the surface. The question then arises of why the kinetics can still be first-order when the average surface coverage of reactants is only a small fraction of the saturation monolayer. We have recently addressed this issue by analyzing the chemisorption geometry of  $\text{CH}_3(\text{ads})$  on Cu(111) with low-energy electron diffraction (LEED) technique. It is found that  $\text{CH}_3(\text{ads})$  tends to form close-packed  $(\sqrt{3} \times \sqrt{3}) \text{R}30^\circ$  structure at all coverages<sup>17</sup> (from  $\theta_{\text{ad}} < 0.2$  to 1 ML, 1 ML defined as one monolayer of adsorbate molecules at saturation coverage). The  $(\sqrt{3} \times \sqrt{3}) \text{R}30^\circ$  structure has also been confirmed by Pascal et al.<sup>18</sup> with the photoelectron diffraction (PhD) method on the same  $\text{CH}_3/\text{Cu}(111)$  system at both saturation and half-saturation coverages. LEED and PhD techniques reflect long-range order and local adsorbate bonding structure. They, however, can only provide rather indirect information on the distribution of adsorbate on the surface. Scanning tunneling microscopy (STM) has been proven to be very powerful for determining surface structure at atomic resolution. To date, there exists no report on probing chemisorbed methyl radicals with STM technique. Here, we present the first result of such study to further resolve the basic problem concerning the adsorption geometry and the chain reaction kinetics.

## Experimental Section

The experiments were carried out in a UHV chamber equipped with a variable-temperature (VT)-STM<sup>19</sup> (Omicron, W-tip, sample temperature control from 20 to over 1000 K) and substrate cleaning, dosing, and annealing attachments. Methyl radicals were generated by pyrolysis of azomethane,

\* Corresponding author. E-mail: chuangtj@ccms.ntu.edu.tw.

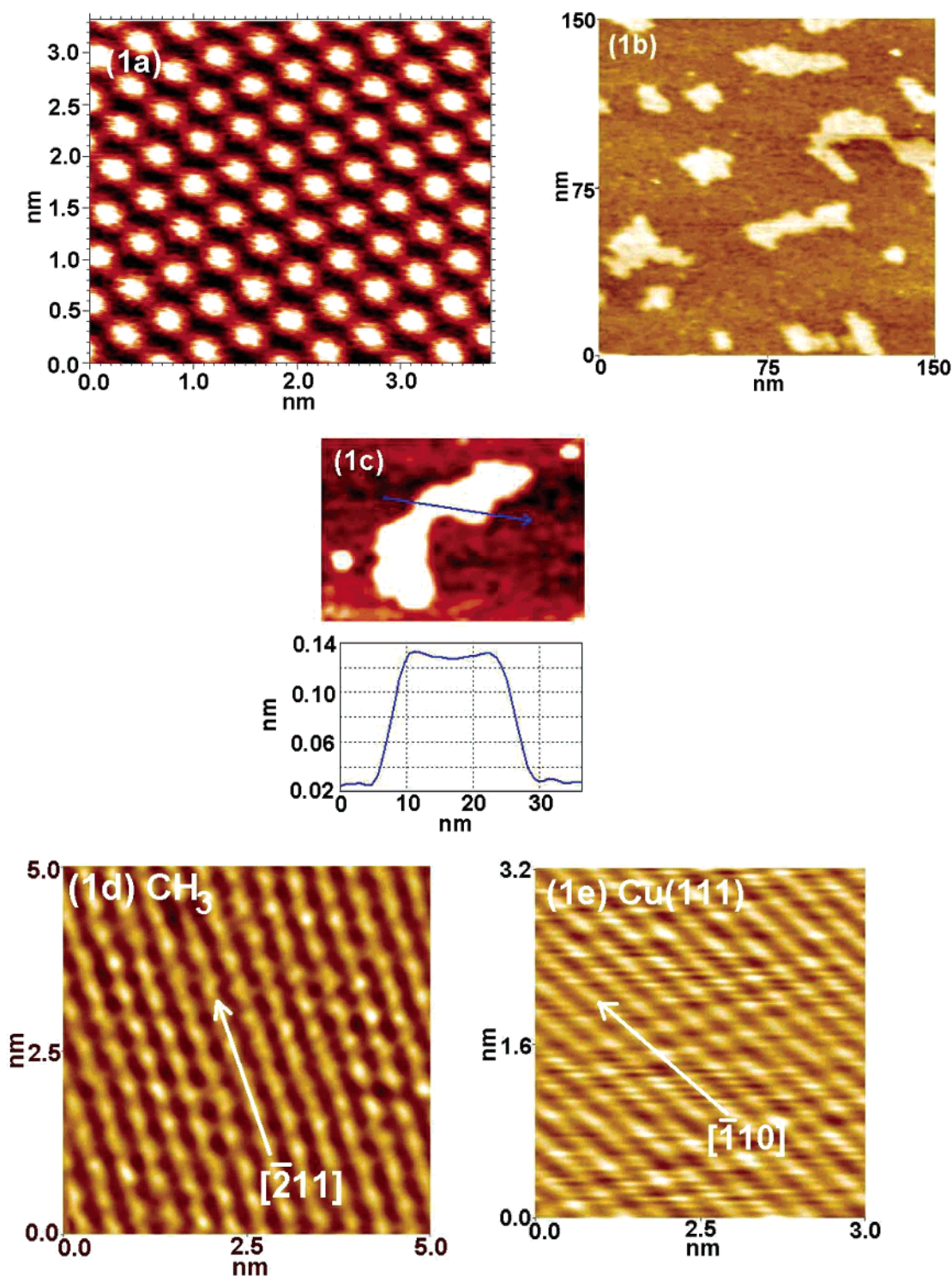


**Figure 1.** STM images of CH<sub>3</sub>(ads)/Cu(111): (a) at  $\theta_{\text{ad}} = 1$  ML saturation coverage and at imaging conditions  $I = 0.14$  nA and sample bias = 0.38 V; (b) at  $\theta_{\text{ad}} = 0.25$  ML submonolayer coverage showing patches of CH<sub>3</sub>(ads) islands on a Cu terrace,  $I = 0.1$  nA, and sample bias = 0.11 V; (c) a step profile across a CH<sub>3</sub>(ads) island as indicated; (d) a pattern of CH<sub>3</sub>(ads) molecules within an island; (e) a CH<sub>3</sub>(ads) island showing the angle between CH<sub>3</sub>(ads) groups along  $[\bar{2}11]$  direction and Cu atomic line in  $[\bar{1}10]$  direction to be about  $30^\circ$ .

and deposition of pure CH<sub>3</sub> on Cu(111) was performed following the procedure as described previously.<sup>20</sup> The gaseous dosing and adsorption characteristics of CH<sub>3</sub>(ads) were analyzed in a separate UHV chamber by X-ray photoelectron spectroscopy (XPS), TPD, LEED, and high-resolution electron energy-loss spectroscopy (HREELS).<sup>16,17,20,21</sup> For STM measurements, typically the CH<sub>3</sub> exposure was conducted at 350 K substrate temperature, so that the maximum surface coverage was never more than one CH<sub>3</sub> monolayer. The sample was then cooled to

60 K for STM imaging. At a given CH<sub>3</sub> exposure and surface coverage, the sample could be annealed at any temperature, but the STM analysis was always performed near 60 K. Images of CH<sub>3</sub> radicals were typically obtained at sample bias voltage of 0.1–0.4 V, depending on specific tip condition. Clear molecule-resolved STM images were difficult to obtain at substrate temperature higher than 300 K for this adsorbate system, possibly due to the increased mobility of CH<sub>3</sub>(ads) and the STM tip-induced effect.

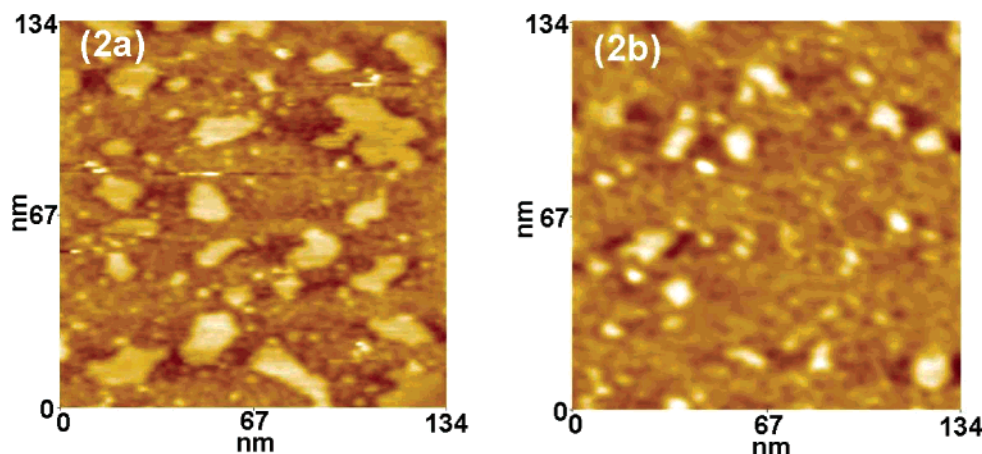


**Figure 2.** STM images of (a) a pattern of  $\text{CH}_3(\text{ads})$  islands at 60 K before thermal treatment and (b) same sample thermally treated at 390 K and then imaged at 60 K.

## Results and Discussion

Figure 1a depicts the STM image of  $\text{CH}_3(\text{ads})$  on Cu(111) at the saturation coverage ( $\theta_{\text{ad}} = 1 \text{ ML}$ ). It exhibits a  $(\sqrt{3} \times \sqrt{3})\text{R}30^\circ$  structure in complete agreement with the LEED data.<sup>17</sup> The PhD analysis<sup>18</sup> and theoretical modeling<sup>22,23</sup> have shown that the radicals reside most likely on the 3-fold hollow sites. The nearest distance between the  $\text{CH}_3(\text{ads})$  groups as determined from Figure 1a is around 4.45 Å, identical to the theoretical value of 4.43 Å with the diameter of Cu atoms at 2.556 Å.<sup>24</sup> With this adsorbate structure, the 2D density ratio between  $\text{CH}_3(\text{ads})$  adlayer and top Cu atoms should be 1:3. This is indeed confirmed by STM. When the clean Cu(111) is exposed to a smaller amount of  $\text{CH}_3$ , the chemisorbed radicals readily form segregated two-dimensional islands with various sizes and shapes. The STM image at  $\theta_{\text{ad}} = 0.25 \text{ ML}$  is displayed in Figure 1b. The step profile of a  $\text{CH}_3$  island is illustrated in Figure 1c. The height of the island with respect to the top Cu surface is about 1.1 Å, and the profile within the island is essentially flat. This step height is quite reasonable for one molecular layer considering the relative sizes of C and H atoms in  $\text{CH}_3$  groups adsorbed in the hollow sites of Cu(111). At a higher STM resolution, the  $\text{CH}_3(\text{ads})$  molecules inside an island and the Cu atoms in the unoccupied surface area are both clearly visible, as exhibited in Figure 1, panels d and e, respectively. From these patterns, we can determine that the line formed by the nearest  $\text{CH}_3$  groups along  $[\bar{2}11]$  direction deviates about  $30^\circ$  from the Cu atomic line in  $[110]$  direction. Moreover, the ratio of distances between the two nearest  $\text{CH}_3$  groups and the Cu atomic row spacing is around 1.80. This length ratio and this line angle are consistent with the  $(\sqrt{3} \times \sqrt{3})\text{R}30^\circ$  chemisorption patterns within the island. This islanding configuration is observed even with  $\theta_{\text{ad}} \ll 1 \text{ ML}$ . From the result, we can conclude that the patches of 2D islands comprise of a close-packed monolayer of  $\text{CH}_3(\text{ads})$  groups.

It is further observed that the sizes of  $\text{CH}_3$  islands become smaller when the sample temperature is raised to 390 K, near the reaction temperature of  $\text{CH}_3(\text{ads})$  groups on Cu(111).<sup>17</sup> The STM images before and after the thermal treatment are depicted in Figure 2a,b. Even though the STM imaging is performed at 60 K, we are certain that the distribution of  $\text{CH}_3(\text{ads})$  is not random at 390 K and methyl group aggregation is maintained. This is inferred from the LEED patterns at 380–420 K<sup>17</sup> in which a weaker, yet nonvanishing  $(\sqrt{3} \times \sqrt{3})$ , local ordering still exists. As mentioned earlier, a clear  $\text{CH}_3(\text{ads})$  image is

difficult to obtain at substrate temperature higher than 300 K. This fact indicates that the adsorbate may be rather mobile and easily perturbed by the STM tip. The 2D islands are likely to be “liquidlike” at such temperature, but apparently the basic  $(\sqrt{3} \times \sqrt{3})$  structure has been upheld according to the LEED data.<sup>17</sup> Because of the relatively low heating rate in the present STM experiment in comparison with the regular TPD measurements, raising the sample temperature to 390 K actually causes some surface reaction to generate high-mass alkyl products. As outlined in the chemical equations, the chain reactions involve the formation of  $\text{CH}_2(\text{ads})$  groups, which then react with intact  $\text{CH}_3(\text{ads})$  to yield  $\text{C}_2\text{H}_5(\text{ads})$ ,  $\text{C}_3\text{H}_7(\text{ads})$ , and  $\text{C}_4\text{H}_9(\text{ads})$  transient surface species.<sup>17</sup> There are two competing reaction channels for the  $\text{C}_{2+}$  transient species to proceed within their surface lifetimes, namely, either to desorb by dehydrogenation or to couple with another  $\text{CH}_2(\text{ads})$  for chain growth. The fact that a high-mass species such as  $\text{C}_4\text{H}_8(\text{g})$  can be produced<sup>17</sup> from a  $\text{CH}_3$  group reacting almost simultaneously with three methylene groups, which are also generated from  $\text{CH}_3(\text{ads})$ , indicates these reagents must be residing almost next to each other even when the average surface coverage is much less than the saturation value. Therefore, at  $\theta_{\text{ad}} \ll 1 \text{ ML}$ , only an aggregated  $\text{CH}_3(\text{ads})$  adsorption structure can support such a chain reaction scheme and explain the observed first-order reaction kinetics. The shrinking of island sizes as the reaction proceeds (Figure 2b) is clearly due to the desorption of reaction products within the islands. Once the products are desorbed, the vacant sites are immediately occupied by the remaining adsorbate forming again the close-packed patterns. It is unlikely that the reduction of island sizes occurs along the perimeters of the islands. Such a reaction–desorption process would result in a fractional-order kinetics with TPD peak shapes and positions strongly dependent on the surface coverage. Since the reactions from  $\text{C}_1$  molecules to yield high mass  $\text{C}_{2+}$  alkyl products with similar first-order kinetics have been observed on a number of solid surfaces, such as Cu(111)<sup>9,10,17</sup>, Cu(100),<sup>11</sup> Cu(110),<sup>12</sup> O/Mo(100),<sup>13,14</sup> and NiO(100),<sup>15</sup> we surmise that the  $\text{CH}_3$  islanding behavior is quite prevalent in these types of catalytic systems.

In conclusion, we provide direct evidence for the formation of 2D islands involving adsorbed methyl radicals on a catalytic surface. The reaction kinetics of the radicals can be correlated with the observed chemisorption geometry. From existing examples, we further infer that the islanding phenomenon of hydrocarbon species may be rather general on catalytic surfaces,



and this type of adsorbate lateral interactions must be considered in pursuing basic understanding of complex reaction mechanisms.

**Acknowledgment.** The authors thank the National Science Council and Ministry of Education of R.O.C. for support of this work.

## References and Notes

- (1) Wintterlin, J.; Volkening, S.; Janssens, T. V. W.; Zambelli, T.; Ertl, G. *Science* **1997**, 278, 1931.
- (2) Trost, J.; Wintterlin, J.; Ertl, G. *Surf. Sci.* **1995**, 329, L583.
- (3) Poirier, G. E. *Langmuir* **1999**, 15, 1167.
- (4) Berner, S.; Brunner, M.; Ramoino, L.; Suzuki, H.; Güntherodt, H.-J.; Jung, T. A. *Chem. Phys. Lett.* **2001**, 348, 175.
- (5) Wintterlin, J. *Advances in Catalysis: Impact of Surface Science on Catalysis*; Academic Press: New York, 2000, pp 131–206.
- (6) Somorjai, G. A. *Chem. Rev.* **1996**, 96, 1223.
- (7) Zaera, F. *Chem. Rev.* **1995**, 95, 2651.
- (8) Bent, B. E. *Chem. Rev.* **1996**, 96, 1361.
- (9) Chiang, C.-M.; Bent, B. E. *Surf. Sci.* **1992**, 279, 79.
- (10) Lin, J.-L.; Bent, B. E. *J. Vac. Sci. Technol., A* **1992**, 10, 2202.
- (11) Lin, J.-L.; Chiang, C.-M.; Jenks, C. J.; Yang, M. X.; Wentzlaff, T. H.; Bent, B. E. *J. Catal.* **1994**, 147, 250.
- (12) Chiang, C.-M.; Wentzlaff, T. H.; Bent, B. E. *J. Phys. Chem.* **1992**, 96, 1836.
- (13) Kim, S. H.; Stair, P. C. *J. Am. Chem. Soc.* **1998**, 120, 8535.
- (14) Kim, S. H.; Stair, P. C. *J. Phys. Chem. B* **2000**, 104, 3035.
- (15) Dickens, K. A.; Stair, P. C. *Langmuir* **1998**, 14, 1444.
- (16) Chuang, P.; Chan, Y. L.; Chien, S.-H.; Klauser, R.; Chuang, T. J. *Chem. Phys. Lett.* **2002**, 354, 179.
- (17) Chuang, P.; Chan, Y. L.; Chien, S.-H.; Song, K.-J.; Klauser, R.; Chuang, T. J. *Langmuir* **2002**, 18, 4549.
- (18) Pascal, M.; Lamont, C. L. A.; Kittel, M.; Hoeft, J. T.; Constant, L.; Polcik, M.; Bradshaw, A. M.; Toomes, R. L.; Woodruff, D. P. *Surf. Sci.* **2002**, 512, 173.
- (19) Pai, W. W.; Hsu, C. L.; Chiang, C. R.; Chang, Y.; Lin, K. C. *Surf. Sci.* **2002**, 519, L605.
- (20) Chuang, T. J.; Chan, Y. L.; Chuang, P.; Klauser, R. *J. Electron. Spectrosc. Relat. Phenom.* **1999**, 98/99, 149.
- (21) Chan, Y. L.; Chuang, P.; Chuang, T. J. *J. Vac. Sci. Technol., A* **1998**, 16, 1023.
- (22) Robinson, J.; Woodruff, D. P. *Surf. Sci.* **2002**, 498, 203.
- (23) Michaelides, A.; Hu, P. *J. Chem. Phys.* **2001**, 114, 2523.
- (24) Winter, M. WebElements Periodic Table. <http://www.webelements.com>. Accessed June 20, 2003.